

New Use for an Old Drug: Inhibiting ABCG2 with Sorafenib

Yinxiang Wei^{1,3}, Yuanfang Ma³, Qing Zhao^{1,4}, Zhiguang Ren^{1,3}, Yan Li¹, Tingjun Hou², and Hui Peng¹

Abstract

Human ABCG2, a member of the ATP-binding cassette transporter superfamily, represents a promising target for sensitizing MDR in cancer chemotherapy. Although lots of ABCG2 inhibitors were identified, none of them has been tested clinically, maybe because of several problems such as toxicity or safety and pharmacokinetic uncertainty of compounds with novel chemical structures. One efficient solution is to rediscover new uses for existing drugs with known pharmacokinetics and safety profiles. Here, we found the new use for sorafenib, which has a dual-mode action by inducing ABCG2 degradation in lysosome in addition to inhibiting its function. Previously, we reported some novel dual-acting ABCG2 inhibitors that showed closer similarity to degradation-induced mechanism of action. On the basis of these ABCG2 inhibitors with diverse chemical structures, we developed a pharmacophore model for identifying the critical pharmacophore features necessary for dual-acting ABCG2 inhibitors. Sorafenib forms impressive alignment with the pharmacophore hypothesis, supporting the argument that sorafenib is a potential ABCG2 inhibitor. This is the first article that sorafenib may be a good candidate for chemosensitizing agent targeting ABCG2-mediated MDR. This study may facilitate the rediscovery of new functions of structurally diverse old drugs and provide a more effective and safe way of sensitizing MDR in cancer chemotherapy. *Mol Cancer Ther*; 11(8); 1693–702. ©2012 AACR.

Introduction

MDR is a major reason for the failure of clinical treatment of cancer and characterized by decreased cellular sensitivities to a broad range of chemotherapeutic agents due, at least mostly, to the overexpression of efflux transport protein on the plasma membrane of cancer cells. Three major human ATP-binding cassette (ABC) transporters have been specialized to play a key role in the clinical development of MDR, including P-glycoprotein (MDR1/ABCB1), MDR protein 1 (MRP1/ABCC1), and breast cancer resistance protein (BCRP/ABCG2; ref. 1). Unlike ABCC1 and ABCB1, human ABCG2 has been considered a half-transporter with a unique arrangement

of its nucleotide-binding domain at the amino terminus and transmembrane at the carboxyl terminus. Human ABCG2 mediates concurrent resistance to the commonly used chemotherapeutic agents, such as mitoxantrone (MX), topotecan, and 7-ethyl-10-hydroxycamptothecin (SN-38), by pumping these drugs out of the tumor cells and thus lowering their cytotoxic effects. Indeed, several clinical studies have clearly shown that ABCG2 overexpression correlates with poor clinical responses in both adult and childhood leukemia patients (2, 3). Therefore, the overexpression of ABCG2 in cancer cells has been an important target of the efficacy of anticancer agents (4).

To date, many ABCG2 inhibitors with diverse chemical structures have been found or developed, but none of them has been tested clinically. It would not be surprising if clinical use of ABCG2 inhibitors with novel chemical structures may have unexpected effects due to several problems, such as toxicity or safety and pharmacokinetic uncertainty of the compound. Although most small molecule tyrosine kinase inhibitors (TKI) are competitive or high-affinity substrates of ABCG2 (5), some of them, such as apatinib (6), sunitinib (7), lapatinib (8), erlotinib (9), gefitinib (10), imatinib (11), nilotinib (12), and vandetanib (13), have been reported to be inhibitors or modulators. These TKIs seem to inhibit the function of ABCG2 transporter by directly interacting with this transporter, thereby completely reversing the MDR of cancer cells (14). Furthermore, the MDR reversal action seems to be unrelated to the expression level of ABCG2. Despite the fact that underlying mechanisms are still not clear, simultaneous administrations of TKIs with chemotherapeutic

Authors' Affiliations: ¹Department of Molecular Immunology, Institute of Basic Medical Sciences, Beijing; ²Institute of Functional Nano & Soft Materials (FUNSOM) and Jiangsu Key Laboratory for Carbon-Based Functional Materials & Devices, Soochow University, Suzhou, Jiangsu; ³Institute of Immunology, Medical School of Henan University, Kaifeng, Henan; and ⁴Medical School of Nankai University, Tianjin, China

Note: Supplementary data for this article are available at Molecular Cancer Therapeutics Online (<http://mct.aacrjournals.org/>).

Y. Wei and Y. Ma contributed equally to this work.

Corresponding Authors: Hui Peng, Department of Molecular Immunology, Institute of Basic Medical Sciences, 27 Taiping Road, Beijing 100850, China. Phone: 86-10-66931326; Fax: 86-10-68159436; E-mail: p_h2002@hotmail.com; and Tingjun Hou, Institute of Functional Nano & Soft Materials (FUNSOM) and Jiangsu Key Laboratory for Carbon-Based Functional Materials & Devices, Soochow University, 199 Ren-ai Road, Suzhou, Jiangsu 215123, China. Phone: 86-512-65882039; E-mail: tjhou@suda.edu.cn or tingjunhou@hotmail.com

doi: 10.1158/1535-7163.MCT-12-0215

©2012 American Association for Cancer Research.

agents, mainly refer to substrates of ABCG2, might be applicable to clinical practice. Regardless, these possibilities are still needed to evaluate effectiveness in the future clinic. Therefore, these joint works for many years have led to further progress in identifying new functions of old drugs already used in the clinic and become one of the practicable solutions in the fast affordable MDR chemosensitizer development.

In our previous studies, we reported, for the first time, a novel dual-acting ABCG2 inhibitor (15), PZ-39, and identified 2 types of ABCG2 inhibitors with one inhibiting only ABCG2 function (static) and the other inducing ABCG2 degradation in lysosome in addition to inhibiting its function (dynamic) (16). The discovery of dynamic inhibitors that induce ABCG2 degradation may, therefore, assist in establishing a new strategy for the reversal of ABCG2-mediated MDR in cancer chemotherapy. In this study, an old drug, sorafenib was identified as a potential ABCG2 inhibitor, showing closer similarity to degradation-induced mechanism of action. On the basis of these reported dynamic ABCG2 inhibitors, we developed a pharmacophore model to identify the critical pharmacophore features necessary for inhibitor-induced ABCG2 degradation. The hypothesis model was also mapped very well with the corresponding functional groups of sorafenib, supporting the argument that sorafenib is a potential ABCG2 dynamic inhibitor. This is the first report that sorafenib may be a good candidate for further evaluation as chemosensitizing agent targeting ABCG2-mediated MDR. This study may facilitate the rediscovery of new functions of structurally diverse old drugs and provide a more effective and safe way of reversing MDR in cancer chemotherapy.

Materials and Methods

Materials

All electrophoresis reagents, protein concentration assay kit, and polyvinylidene difluoride membranes were purchased from Bio-Rad. Adriamycin, topotecan, and mitoxantrone were from Zhejiang Hisun Pharmaceutical Co., Ltd., Huangshi Feiyun Pharmaceutical Co., Ltd., and Jiangsu Hansoh Pharmaceutical Co., Ltd., respectively. Rhodamine-123, Ko143, SRB, bafilomycin A1, and MG-132 were obtained from Sigma-Aldrich. Monoclonal antibody (mAb) C-219 against ABCB1 and BXP-21 against ABCG2 were purchased from Abcam. MRPr1 against ABCC1 was from ARP American Research Products, Inc. Anti-AKT, p-AKT, ERK1/2, and p-ERK1/2 antibodies were acquired from Cell Signaling. PE-conjugated 5D3 antibody was from eBiosciences. Real-time PCR Master Mix was purchased from TOYOBO. Dimethyl sulfoxide (DMSO), TRIZOL, and G418 were purchased from Invitrogen. Cell culture medium RPMI-1640 and Dulbecco's Modified Eagle's Medium were purchased from HyClone. Sorafenib standard was purchased from J&K Scientific Ltd. All other chemicals were obtained from commercial sources of analytical grade.

Cell culture, treatments, and lysate preparations

The human chronic myelogenous leukemia cell line K562 and its drug-selected cell line K562/A02 (17) were kindly provided by Prof. Dongsheng Xiong (Institute of Hematology & Blood Diseases Hospital, CAMS & PUMC, China). HEK293-transfected sublines HEK293/Vec (18), HEK293/ABCC1 (19), and HEK293/ABCG2 (20) were obtained from Prof. Jian-ting Zhang (Indiana University Simon Cancer Center, Indianapolis, IN). The human breast cancer cell line MCF-7 and the mitoxantrone selected MDR cell line MCF-7/MX (21) were kindly provided by Dr. E. Schneider (Wadsworth Center, Albany, NY). All cell lines from gifts were cultured as previously described and frozen into multiple aliquots. All cells were passaged for 4 months or less before the renewal from frozen, early-passage stocks. All cell lines were periodically authenticated by morphologic inspection. For analysis of ABCG2 degradation, HEK293/ABCG2 cells were first treated with 10 nmol/L bafilomycin A1 or 2 μ mol/L MG-132 for 24 hours followed by treatment with 2.5 μ mol/L sorafenib for 3 days and collection of cell lysates. Lysate preparation was carried out as described previously (15).

Western blot and fluorescence-activated cell sorting analyses

Western blot and fluorescence-activated cell sorting (FACS) analyses of drug accumulation were carried out exactly as we previously described (15, 20). To determine the conformational change of ABCG2 following treatment with ABCG2 inhibitors, HEK293/ABCG2 cells were incubated with 0.5 and 2.5 μ mol/L sorafenib at 37°C for 10 minutes before PE-conjugated 5D3 antibody (1:20 dilution) was added and incubated for 30 minutes. The cells were then washed 3 times and analyzed by FACS.

Real-time reverse transcriptase-PCR and cytotoxicity assay

RNA extraction and real-time reverse transcriptase PCR (RT-PCR) were carried out as we described previously (15). The sequences of ABCG2 primers are 5'-TCAT-CAGCCTCGATATTCCATCT-3' (forward) and 5'-GGC-CCGTGGAACATAAAGTCTT-3' (reverse). The sequences of glyceraldehyde-3-phosphate dehydrogenase (GAPDH) primers are 5'-CCGTCTAGAAAAACCTGCC-3' (forward) and 5'-GCCAAATTCGTTGTCATACC-3' (reverse). The standard curve and data analysis were produced using Bio-Rad iQ5 software. The relative ABCG2 mRNA level treated with inhibitors was expressed as fold change of the control (in the presence of 0.1% DMSO).

Cytotoxicity was determined using SRB and MTS assays as previously described (15, 16). The effect of inhibitors on drug resistance was determined by exposing cells to a low concentration (\leq IC₁₀) of anticancer drugs, such as adriamycin, mitoxantrone, and topotecan, in the absence or presence of different concentrations of sorafenib.

Drug accumulation and *in vitro* transport assays

Drug accumulation assay was carried out as described previously (15, 16) with some modifications. Briefly, 10^6 cells in culture were preincubated with various concentrations of sorafenib, Ko143, verapamil, or vehicle control (0.1% DMSO) for 1 hour at 37°C, followed by addition of 20 $\mu\text{mol/L}$ mitoxantrone and incubation for 30 minutes. The reaction was stopped by addition of ice-cold PBS and centrifugation, washed with ice-cold PBS 3 times, and subjected analysis flow cytometry.

Inhibition kinetics of sorafenib on intracellular mitoxantrone (ABCG2 substrate) efflux by ABCG2 was detected as previous described (6). Briefly, HEK293/ABCG2 cells were incubated with mitoxantrone (2.5–20 $\mu\text{mol/L}$ in final) at 37°C for 30 minutes. The cells were centrifuged, collected, washed once with cold PBS, and resuspended in medium with free mitoxantrone in the presence or absence of 2.5 $\mu\text{mol/L}$ sorafenib. Then, the cells were incubated at 37°C for 10 minutes, centrifuged, and washed at least 2 times with cold PBS. The apical uptake reaction kept at 0°C was taken as control. The intracellular concentration of drug was determined by FACS. The quantity of drug efflux by ABCG2 was calculated by subtracting the values obtained at 37°C from those at 0°C. The inhibitory effect of sorafenib was analyzed using Lineweaver–Burk plots as previously described (6).

Pharmacophore modeling

The common pharmacophore features among 4 dynamic ABCG2 inhibitors (PZ-8, 34, 38, and 39) reported by us were generated by LigandScout (version 3.0). Diverse conformations for each compound were generated such that the conformers covered accessible conformational space defined within 10 kcal/mol of the estimated global minimum. Then, the ligand-based pharmacophore creation workflow in LigandScout was used to identify configurations or 3-dimensional (3D) spatial arrangements of chemical features that are common to molecules in a training set. In this work, 4 kinds of chemical features, including hydrogen bond acceptor (HBA), hydrogen bond donor (HBD), hydrophobic center, and aromatic ring, were used in pharmacophore modeling. The maximum number of chemical features in each hypothesis was set to 10, and the maximum number of pharmacophore hypotheses was set to 10. Finally, the best pharmacophore hypothesis was used to evaluate how well sorafenib can be mapped with pharmacophore model.

Results

Effect of sorafenib on ABCG2-mediated mitoxantrone accumulation

To investigate the effect of sorafenib on ABCG2-mediated drug efflux, mitoxantrone was used as a model substrate. Intracellular mitoxantrone accumulation in ABCG2 R482G-transfected stable HEK293 (HEK293/ABCG2) cells and its corresponding ABCG2-negative vector-transfected control (HEK293/Vec) cells were mea-

sured in the presence or absence of sorafenib or Ko143 at 2.5 $\mu\text{mol/L}$. As shown in Fig. 1A, sorafenib and Ko143 produced a significant increase of mitoxantrone accumulation in HEK293/ABCG2, but little effects on HEK293/Vec. The preincubation of cells with sorafenib and Ko143 also enhanced intracellular mitoxantrone accumulation in MCF7/MX that overexpress wild-type ABCG2 but not in the parental MCF7/WT cells (Supplementary Fig. S1), indicating that the effect of sorafenib on mitoxantrone accumulation is likely via inhibiting ABCG2. Then we determined the concentration-dependent effect of sorafenib on ABCG2-mediated mitoxantrone accumulation in HEK293/ABCG2 cells by flow cytometry. As shown in Fig. 1B, the mitoxantrone accumulation in the absence of sorafenib was remarkably decreased in ABCG2-overexpressing cells, as compared with that in its corresponding ABCG2-negative cells (shadow peak). Addition of sorafenib increased the intracellular mitoxantrone level in ABCG2-overexpressing cells in a dose-dependent manner. The value of IC_{50} for sorafenib inhibition of ABCG2-mediated drug efflux was approximately 1.31 $\mu\text{mol/L}$ (Supplementary Fig. S4).

To further investigate the specificity of sorafenib, we tested its effect on drug efflux mediated by 2 other major MDR-related ABC (MDR-ABC) transporters that are known to cause MDR, ABCB1, and ABCC1 using K562 drug-selected resistant cells that overexpress ABCB1 (K562/A02) and HEK293 cells that were transfected with ABCC1 (HEK293/ABCC1). However, we found no effect of sorafenib on the activity of ABCB1 and ABCC1 in decreasing rhodamine-123, adriamycin accumulation, respectively (Fig. 1C and D). Thus, although the structure of sorafenib is different to previously reported ABCG2 inhibitors, it seems to be specific to ABCG2 and do not affect drug efflux mediated by 2 other major MDR-ABC transporters (up to 2.5 $\mu\text{mol/L}$ concentration in this study).

Sensitization of sorafenib on ABCG2-mediated MDR

To determine whether sorafenib has the ability to sensitize ABCG2-mediated drug resistance, we carried out analyses of the effect of sorafenib at nontoxic dose on the survival of HEK293/ABCG2 and HEK293/Vec cells in the absence or presence of different well-known ABCG2 substrates, including mitoxantrone and topotecan. As shown in Fig. 2, we found that sorafenib alone is not cytotoxic with a concentration up to 2.5 $\mu\text{mol/L}$ (high dose in Fig. 2) on the survival of parental and resistant cells. But in the combined application of sorafenib and anticancer drugs, which alone have less than 10% inhibition of growth of cells, sorafenib produced a chemosensitivity increase of ABCG2 substrates in a dose-dependent manner in the HEK293/ABCG2, whereas it had little influence on the parental HEK293/Vec cells (Fig. 2A and B). Supplementary Fig. S2 also showed that sorafenib significantly potentiated the toxicity of mitoxantrone in MCF7/MX (wild-type ABCG2) cells, though sorafenib alone was not cytotoxic to parental MCF7/WT and

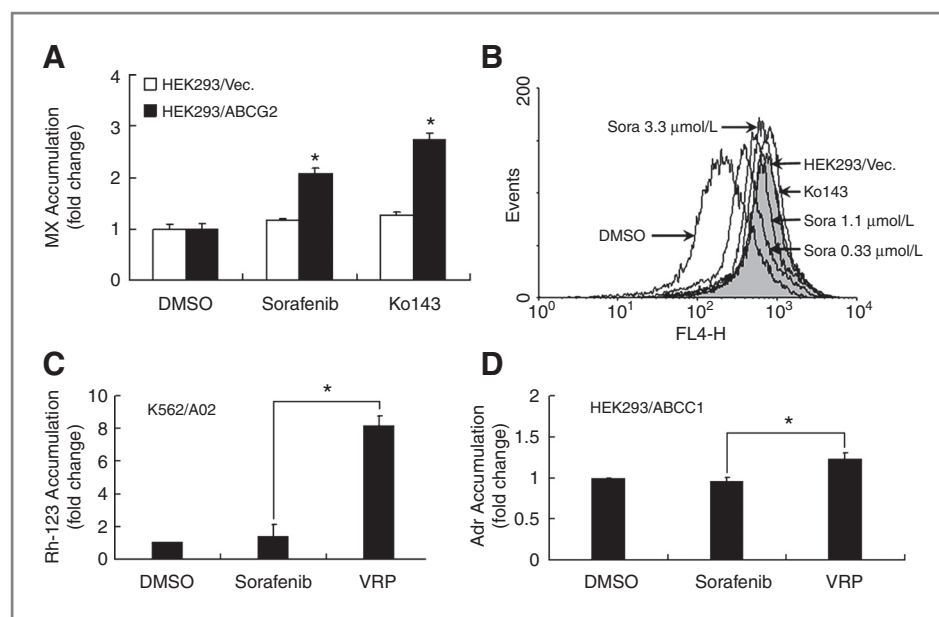


Figure 1. Effect of sorafenib on the intracellular substrate accumulation. **A**, mitoxantrone accumulation in HEK293 cells transfected with vector (HEK293/Vec) or ABCG2 (HEK293/ABCG2) following a 30-minute incubation in the absence or presence of sorafenib or Ko143 (2.5 $\mu\text{mol/L}$). The data are means \pm SD from 3 independent experiments (*, $P < 0.01$, compared with DMSO vehicle). **B**, dose response of sorafenib in restoring mitoxantrone accumulation in HEK293/ABCG2 cells. The shadow peak shows the level of mitoxantrone accumulation in vector-transfected cells, serving as a control. Ko143 (2.5 $\mu\text{mol/L}$) was also used as a positive control. The data are representative of 3 independent experiments. **C** and **D**, Rh-123 accumulation in K562/A02 cells overexpressing ABCB1 (**C**) or adriamycin accumulation in HEK293/ABCC1 cells overexpressing ABCC1 (**D**) following a 30-minute incubation in the absence or presence of sorafenib (2.5 $\mu\text{mol/L}$) or verapamil (10 $\mu\text{mol/L}$). Verapamil (VRP) was used as a positive control. The data are means \pm SD from 3 independent experiments (*, $P < 0.01$, sorafenib compared with verapamil control).

MCF7/MX cells, supporting the argument that sorafenib is a potent ABCG2 inhibitor. We next determined the specificity of sorafenib on the survival of K562/A02 and HEK293/ABCC1 that overexpress human ABCB1 and ABCC1, respectively. As shown in Fig. 2C and D, sorafenib at the same concentration did not significantly alter the cytotoxicity of adriamycin, both as the substrate of ABCB1 and ABCC1, in K562/A02 and HEK293/ABCC1 cells, supporting the above notion that sorafenib (up to 2.5 $\mu\text{mol/L}$) may be specific to ABCG2 and do not affect MDR mediated by ABCB1 and ABCC1 transporters.

Interaction of sorafenib and ABCG2

As reported previously, mAb 5D3 recognizes and binds to ABCG2 on the cell surface more readily in the presence of ABCG2 inhibitors possibly due to inhibitor-induced conformational changes of ABCG2 (15, 22). To detect whether sorafenib can bind to ABCG2, we carried out staining analyses of ABCG2 using 5D3 in the presence or absence of sorafenib in HEK293/ABCG2 cells. As shown in Fig. 3A, sorafenib caused an increase of 5D3 staining in HEK293/ABCG2 cells, supporting the possibility that sorafenib directly binds to ABCG2 and leads to ABCG2 conformational changes.

To further understand the mechanism of action underlying inhibition of ABCG2-mediated transport by sorafenib, we tested the effect of sorafenib on the kinetics of the intracellular mitoxantrone efflux mediated by ABCG2 transporter using HEK293/ABCG2 cells. The fluores-

cence change of mitoxantrone was determined in the presence or absence of sorafenib using flow cytometry. As shown in the Lineweaver-Burk plot (Fig. 3B), sorafenib was a noncompetitive inhibitor of mitoxantrone efflux. Thus, our study showed that sorafenib binds to a different site on ABCG2 from mitoxantrone, not being a competitive inhibitor of mitoxantrone.

Dual action of sorafenib on ABCG2

To determine whether sorafenib has the dual-acting characteristic, we also tested the effect of sorafenib on ABCG2 expression using Western blot analysis. As shown in Fig. 4A, sorafenib dramatically decreased the expression of ABCG2 in both concentration- and time-dependent manners, the results are similar to those of PZ-38 that was used as a positive control (Fig. 4B). As previously described, after incubating resistant cells for 2 hours, sorafenib was able to inhibit ABCG2-mediated mitoxantrone efflux, whereas ABCG2 expression decreased only marginally in drug-resistant cells. A significant decrease in the ABCG2 protein level was observed at day 1 after sorafenib treatment. The similar effects were also observed in MCF7/MX that overexpresses wild-type ABCG2 cells (Supplementary Fig. S3). However, as shown in Fig. 4C, the well-known ABCG2 inhibitor Ko143 does not affect ABCG2 expression level, although both sorafenib and Ko143 significantly increased mitoxantrone accumulation in HEK293/ABCG2 cells. To determine the specificity of sorafenib, we also tested the effect of

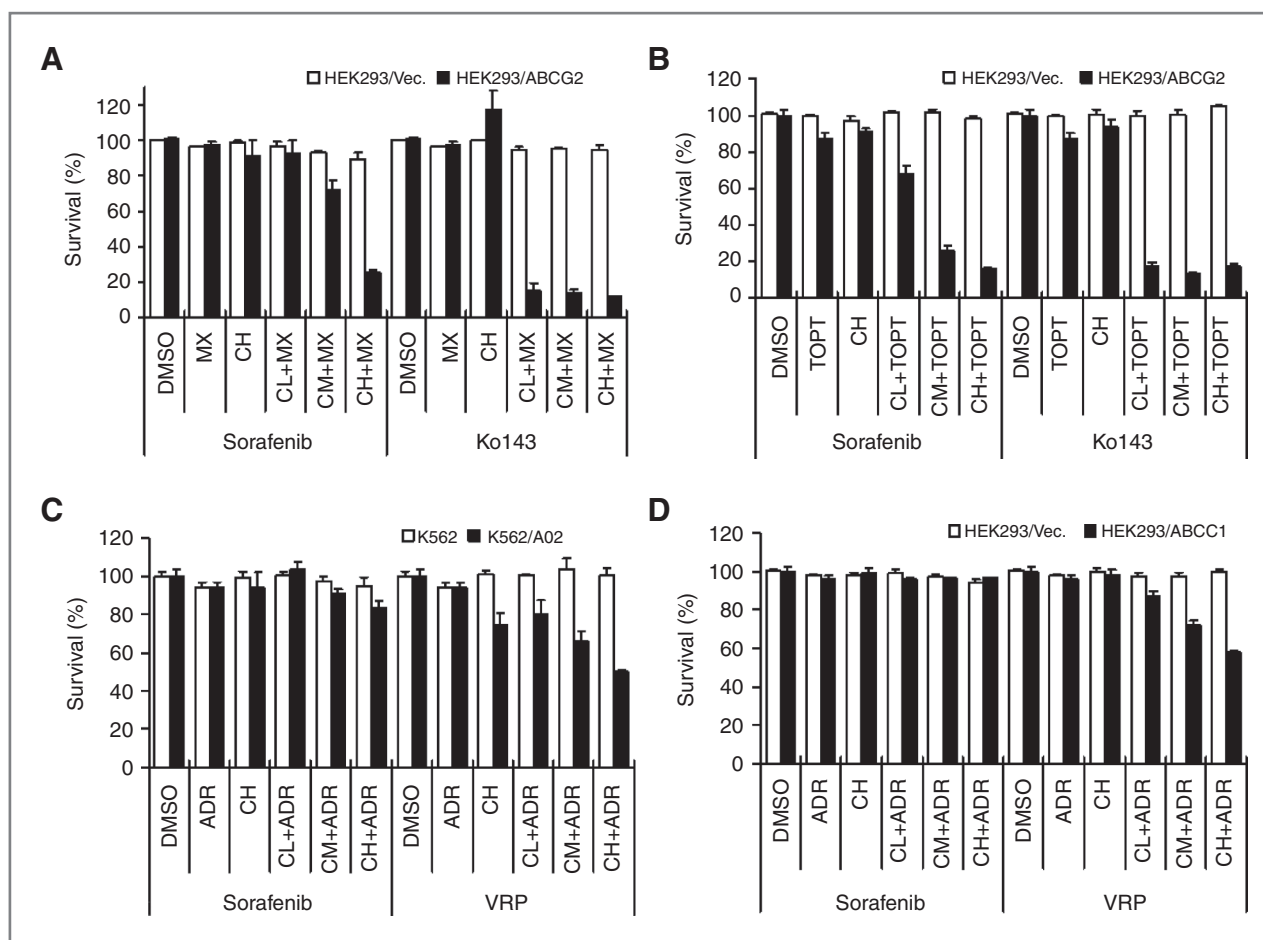


Figure 2. Chemosensitization of drug resistance by sorafenib. A and B, HEK293/Vec (open bar) or HEK293/ABCG2 (filled bar) cells were treated with or without IC₁₀ of mitoxantrone (A) and topotecan (B) in the absence or presence of different concentrations of sorafenib (CH, 2.5 μ mol/L; CM, 1.25 μ mol/L; CL, 0.625 μ mol/L) followed by SRB assay. C and D, K562 (open bar) and K562/A02 (filled bar) that overexpress ABCB1 (C) or HEK293/Vec (open bar) and HEK293/ABCC1 (filled bar) that were transfected with ABCC1 (D) cells were treated with or without IC₁₀ of adriamycin in the absence or presence of different concentrations of sorafenib (CH: 2.5 μ mol/L; CM: 1.25 μ mol/L; CL: 0.625 μ mol/L) followed by MTS assay. Ko143 was used as an ABCG2 inhibitor control, whereas verapamil (VRP) was used as a positive control of ABCB1 and ABCC1. The results are presented as survival rate of MDR cells relative to DMSO vehicle and shown as means \pm SD of 3 independent experiments.

sorafenib on the steady-state protein level of ABCB1 and ABCC1. The expression of ABCB1 and ABCC1 proteins was not affected by treating drug-resistant cells with 2.5 μ mol/L sorafenib for 3 days, compared with vehicle control (0.1% DMSO; Fig. 4D). Thus, sorafenib is likely specific to ABCG2 among 3 major MDR-ABC transporters that are believed to be involved in clinical drug resistance.

To examine whether sorafenib causes ABCG2 degradation via the lysosome or proteasome, we used bafilomycin A1, an inhibitor of protein degradation in lysosome, and MG-132, a proteasome inhibitor as previously described (15). As shown in Fig. 5A, cotreatment of cells with bafilomycin A1 inhibited sorafenib-induced ABCG2 degradation, whereas cotreatment with MG-132 did not. Similar to PZ-series dynamic inhibitors, as previously reported, sorafenib likely induced ABCG2 degradation in the lysosome. Taken together, we concluded that sorafenib seems to have dual actions by inhibiting ABCG2

function and by inducing ABCG2 degradation in the lysosome.

To determine whether the effect of sorafenib on ABCG2 expression is at the mRNA level, we carried out real-time RT-PCR analysis of HEK293/ABCG2 cells treated with 2.5 μ mol/L sorafenib for various times up to 3 days. As shown in Fig. 5B, no significant changes in ABCG2 mRNA level were found. We assumed that the mechanism of sorafenib-mediated inhibition would be at the posttranscriptional level.

The most extensively studied receptor tyrosine kinases (RTK) mainly refer to the members of the EGFR, VEGFR, c-KIT, FLT-3, and PDGFR, several of which are thought to be involved in sorafenib treatment. Two major downstream signaling pathways stimulated by RTKs include the Ras/Raf/MEK/ERK and PI3K/AKT pathways that play a central role in proliferation and survival of cancer cells. It has also been reported previously that resistance to

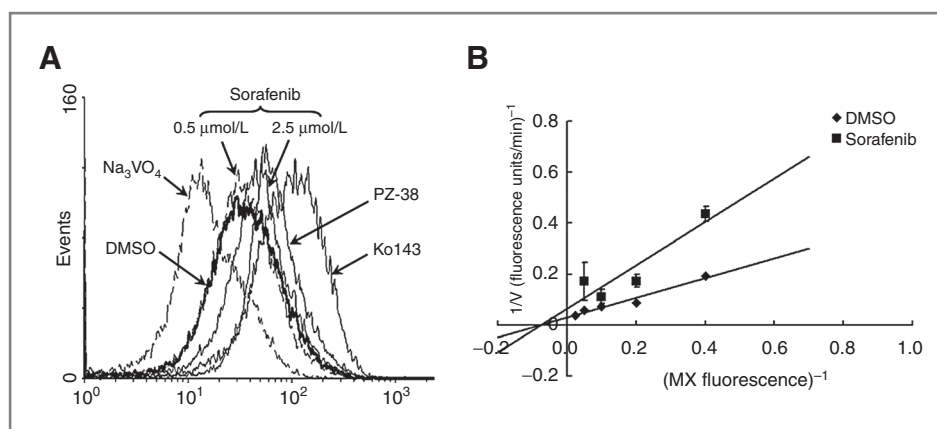


Figure 3. Effect of sorafenib on ABCG2 conformational change and the transport kinetics of substrate. **A**, effect of sorafenib on 5D3 staining of ABCG2. HEK293/ABCG2 cells were treated with DMSO vehicle control, 1 mmol/L Na_3VO_4 , 10 $\mu\text{mol/L}$ PZ-38 or Ko143, 0.5 and 2.5 $\mu\text{mol/L}$ sorafenib followed by staining with mAb 5D3 and FACS analysis. PZ-38 and Ko143 were used as ABCG2 inhibitor-induced conformational changes control. The data are representative of 3 independent experiments. **B**, effect of sorafenib on the transport kinetics of ABCG2-mediated intracellular mitoxantrone efflux. The quantity of mitoxantrone efflux in HEK293/ABCG2 cells was measured for 10 minutes at 37°C at various mitoxantrone concentrations (2.5–20 $\mu\text{mol/L}$) in the absence (\blacklozenge) or presence (\blacksquare) of 2.5 $\mu\text{mol/L}$ sorafenib by flow cytometry. The points are means \pm SD from 3 independent experiments.

some anticancer drugs in cancer cells can be decreased by inhibiting the AKT and ERK1/2 pathways (23, 24). To investigate the effect of sorafenib on ABCG2 via the suppression of the AKT and ERK1/2 protein activity, we examined the change of total and phosphorylated forms of AKT and ERK1/2 after treatment with sorafenib at ABCG2 reversal concentration in both the resistant and parental cells. As shown in Fig. 5C, the incubation of cells with sorafenib (2.5 $\mu\text{mol/L}$) for 3 days did not effectively change the total and phosphorylated forms of AKT and ERK1/2 in all cell lines tested. It suggested that the ABCG2-mediated MDR reversal effect by sorafenib is independent of the inhibition of the AKT and ERK1/2 proteins.

Validation of sorafenib by the pharmacophore hypothesis

Previously, we reported that the rational screening of representatives of different types of compound library resulted in identification of some dual-mode acting ABCG2 dynamic inhibitors, such as PZ-8, PZ-34, PZ-38, and PZ-39 (16). Their chemical structures are shown in Fig. 6A, which are structurally different from sorafenib. To verify the new functions of sorafenib, we developed a pharmacophore model for dynamic ABCG2 inhibitors by LigandScout. From the calculated results, it can be found that the best pharmacophore hypothesis (Fig. 6B), based on the 4 PZ series compounds, has 6 features, including 3 HBA, 2 hydrophobic centers, and

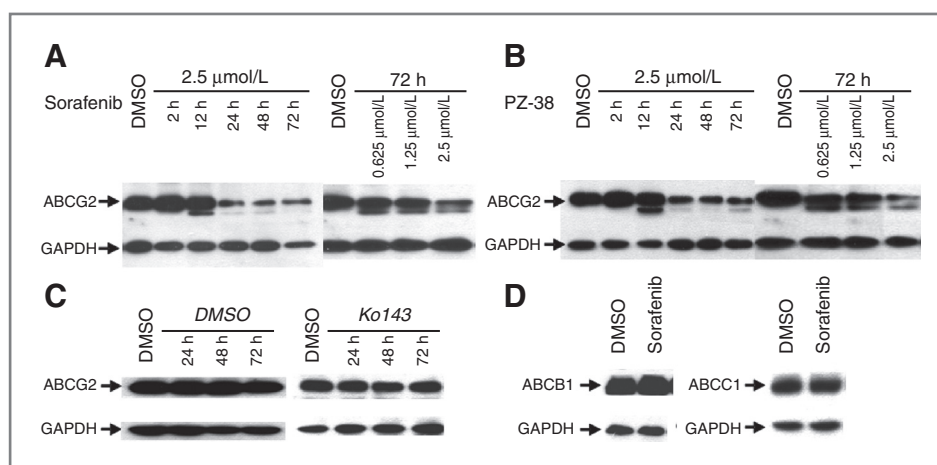


Figure 4. Effect of sorafenib on human ABCG2 expression level. **A–C**, HEK293/ABCG2 cells were treated with sorafenib (**A**), PZ-38 (**B**), DMSO vehicle, and Ko143 (**C**) in dose- and time-dependent manner followed by Western blot analysis for ABCG2 expression. PZ-38 was chosen to be a positive control, whereas 0.1% DMSO and 2.5 $\mu\text{mol/L}$ Ko143 were used as negative control. **D**, K562/A02 cells with ABCB1 overexpression and HEK293/ABCC1 cells were treated with 0.1% DMSO or 2.5 $\mu\text{mol/L}$ sorafenib for 3 days followed by Western blot analysis of ABCB1 using mAb C219 and ABCC1 using mAb MRP1. GAPDH was used as a loading control. The data are representative of 3 independent experiments.

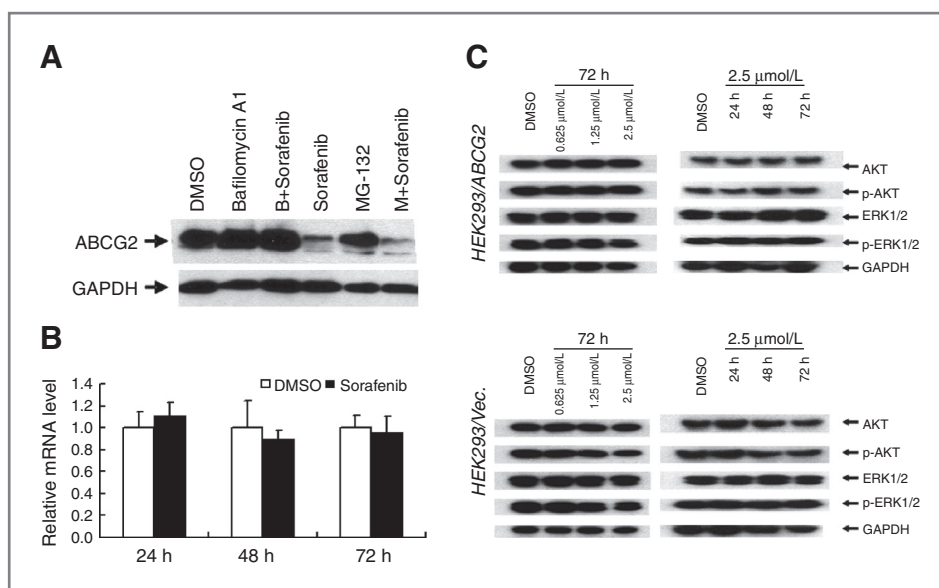
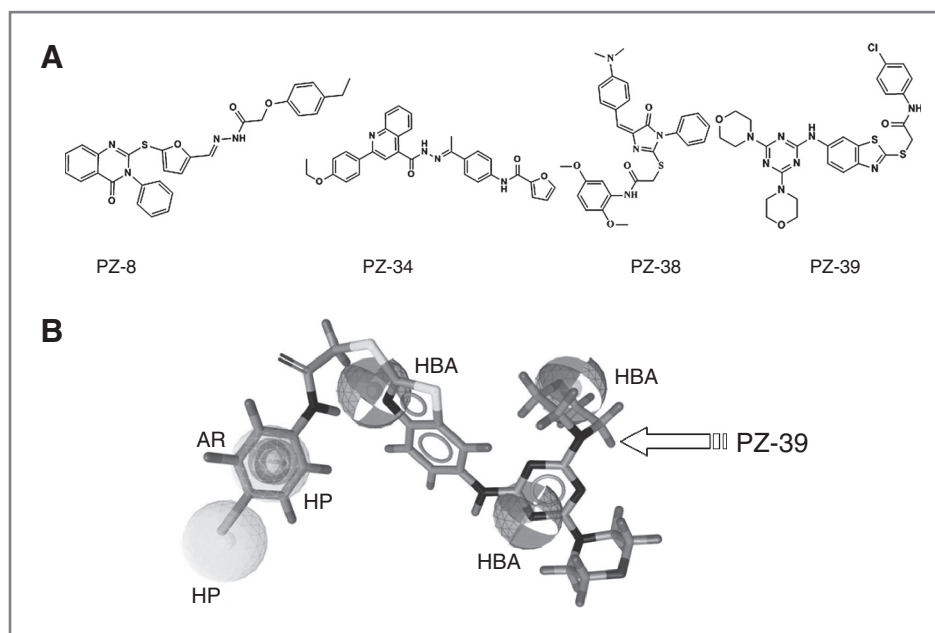


Figure 5. Effect of sorafenib on ABCG2 degradation, mRNA level, and the phosphorylation of AKT and ERK1/2. **A**, effect of bafilomycin A₁ and MG-132 on sorafenib-induced ABCG2 degradation. HEK293/ABCG2 cells were treated with 2.5 μmol/L sorafenib in the absence or presence of 10 nmol/L bafilomycin A₁ or 2 μmol/L MG-132 for 3 days and harvested for Western blot analysis of ABCG2 expression. GAPDH was used as a loading control in all Western blot analyses. **B**, effect of sorafenib on ABCG2 mRNA level. HEK293/ABCG2 cells were treated with DMSO vehicle (open bar) or 2.5 μmol/L sorafenib (filled bar) for various times and harvested for RNA preparation and real-time RT-PCR analysis. Data shown are mean ± SD from 3 independent experiments. **C**, effect of sorafenib on the phosphorylation of AKT and ERK1/2. HEK293/Vec or HEK293/ABCG2 cells were treated with sorafenib or DMSO vehicle in dose- and time-dependent manner followed by Western blot analysis for expression of AKT, p-AKT, ERK1/2, and p-ERK1/2. GAPDH was used as a loading control. The data are representative of 3 independent experiments.

one aromatic center. Figure 6B also depicts the most active conformation of compound PZ-39 superimposed on the best pharmacophore hypothesis, indicating that the hypothesis can be well mapped by the corresponding functional groups of PZ-39. It seems that the hydrophobic interactions and the hydrogen-bonding interactions are essential for ligand binding. Then, sorafenib was

further evaluated by the best pharmacophore hypothesis. The 3D alignment of sorafenib with the pharmacophore hypothesis was shown in Fig. 7A. Sorafenib forms impressive alignment with the pharmacophore hypothesis. The detailed 2D mapping of the pharmacophore hypothesis with the structural features of sorafenib is depicted in Fig. 7B. From Fig. 7A and B, we can see that

Figure 6. Chemical structures of dual-acting ABCG2 inhibitors and alignment of most active compound with the pharmacophore hypothesis. **A**, chemical structures of PZ-8, PZ-34, PZ-38, and PZ-39. **B**, the alignment of PZ-39 with the pharmacophore hypothesis. HBA, hydrogen bond acceptor; HP, hydrophobic center; AR, aromatic ring.



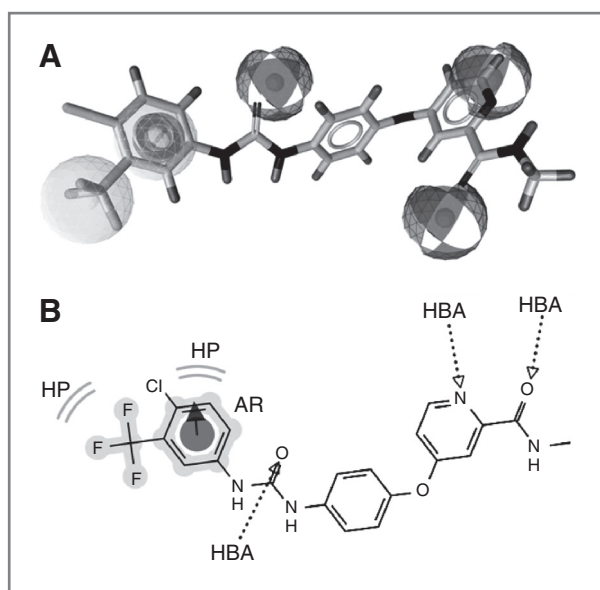


Figure 7. The 2D and 3D alignment of sorafenib with the pharmacophore hypothesis. **A**, the 3D alignment of sorafenib with the pharmacophore hypothesis. **B**, the 2D representation of the structural features in sorafenib that can be aligned with the pharmacophore hypothesis. HBA, hydrogen bond acceptor; HP, hydrophobic center; AR, aromatic ring.

the aromatic center of pharmacophore hypothesis was mapped onto the phenyl ring of sorafenib, and the 2 hydrophobic centers of pharmacophore hypothesis mapped onto the same phenyl ring and substituted trifluoromethyl group. With regard to the 3 hydrogen bond acceptor features, one was mapped onto the O-atom of ureido group of sorafenib, another one onto the N-atom of pyridine ring, and the third onto O-atom of benzene sulfonate group. From here, we can conclude that the chemical features described in the pharmacophore hypothesis are consistent with the corresponding functional groups of sorafenib. Therefore, it is possible that sorafenib may be a potential ABCG2 dynamic inhibitor, which has a dual-mode action by inducing ABCG2 degradation in lysosome and by inhibiting its function.

Discussion

Previously, we reported that there are possibly 2 groups of ABCG2 inhibitors with one inhibiting ABCG2 function (static inhibitor) and the other not only inhibiting ABCG2 activity but also inducing ABCG2 degradation (dynamic inhibitor; ref. 16). Therefore, there is a widespread interest in elucidating whether some existing drugs are ABCG2 dynamic inhibitors. With this aim, sorafenib was rediscovered to be a potent ABCG2 dynamic inhibitor *in vitro*. Moreover, a chemical feature based on 3D pharmacophore model of ABCG2 degradation-induced inhibitors has been developed and mapped very well with the corresponding functional groups of sorafenib, supporting the above notion. Although sorafenib is structurally different from our previously reported ABCG2 degradation-

induced inhibitors, our results suggest, for the first time, that sorafenib has a similar action to the dynamic inhibitor, namely, not only inhibiting ABCG2 function but also inducing ABCG2 degradation in the lysosome.

Recent reports have revealed the evidences of interaction between sorafenib and MDR-ABC transporters. Sorafenib has been shown to be recognized and effluxed by both ABCB1 and ABCG2. Agarwal and colleagues reported that ABCG2 has higher affinity for sorafenib than ABCB1 and play a dominant role in the efflux of sorafenib at the BBB *in vivo* study (25). Lagas and colleagues confirmed that brain efflux of sorafenib is more efficiently transported by ABCG2 with playing the dominant role in limiting its brain accumulation by murine *Abcg2* (26). Among these publications, none of them shows that sorafenib is an inhibitor of the ABCG2 transporter. Hu and colleagues reported that sorafenib was able to decrease Hoechst 33342 (a substrate of ABCG2) efflux in the ABCG2-overexpressing cells by IC_{50} of approximately 3.1 $\mu\text{mol/L}$ (27), supporting our claim that at a concentration of 2.5 $\mu\text{mol/L}$, sorafenib drastically reverses ABCG2-mediated drug substrates efflux. However, it is not clear whether sorafenib acts as an ABCG2 inhibitor. In another study, using *in vitro* model of stably transduced MDCKII cell lines with human ABCB1 and ABCG2, Poller and colleagues reported that ABCG2 was the major contribution to transport sorafenib at 0.3 $\mu\text{mol/L}$ and began saturation at 2.0 $\mu\text{mol/L}$ (28). In our study, sorafenib completely achieved the level of inhibition at 2.5 $\mu\text{mol/L}$ compared with saturated concentration at 2.0 $\mu\text{mol/L}$ on the ABCG2-binding site. Clearly, the above mentioned results are not only consistent with our ATPase result in which sorafenib is a substrate of ABCG2 (Supplementary Table S1), but their data are also in agreement with our finding that sorafenib serves as a substrate of the ABCG2 transporter at a low concentration, while saturating all the binding sites, it can inhibit the transporter at high concentrations. In a review of protein kinase inhibitors (PKI) and ABC transporters (29), Hegedüs and colleagues drew the same conclusion as ours: a modulator is a substrate or an inhibitor of an MDR-ABC transporter may depend on actual drug concentrations. Supposedly, an anticancer small molecule PKI may be a MDR-ABC transporter substrate, the PKI is directly extruded by the MDR-ABC transporter in an ATP-dependent fashion at a low PKI level, whereas the transporter is often inhibited at a high PKI concentration. On the whole, these data suggest that sorafenib may interact with ABCG2, and the combined therapy of sorafenib and ABCG2 substrates may affect the pharmacokinetics of these anticancer drug substrates.

In the human pharmacokinetic studies, the mean peak plasma level of sorafenib was approximately 13.5 $\mu\text{mol/L}$ (6.2 $\mu\text{g/mL}$) with a mean half-life of 35 hours in patients with advanced solid tumors (30). These data suggest that the *in vitro* concentration of sorafenib (2.5 $\mu\text{mol/L}$, used in our experiments) is much lower than those obtained in the plasma after therapeutic treatment, and it has

considerable potential of ideal chemosensitizer that should not be toxic itself. Thus, it is possible that sorafenib behaves like chemosensitizing agent of resistant cancer cells through its interaction with ABCG2 transporter. However, it is unknown whether sorafenib is effective in reversing ABCG2-mediated MDR *in vivo*, although its concentration is not toxic *in vitro*. Regardless, these possibilities need to be evaluated in the future studies using animal models.

Sorafenib shares with PZ-series dynamic inhibitors in a similar action without any apparent structural similarities. The identification of a common pharmacophore for PZ-series dynamic inhibitors presented here is a valuable example of molecular modeling that help us to evaluate how well diverse old drugs can be mapped with the pharmacophore before experimental study. The unification of PZ-compounds in a single pharmacophore provides a framework to study ABCG2-inhibitor interactions that should assist in the rational design of inhibitors inducing ABCG2 degradation. However, the precise structure-activity relationship and refined pharmacophore model remain to be elucidated when more ABCG2 dynamic inhibitors will be available in the near future.

In summary, we show, for the first time, that nontoxic dose of sorafenib may inhibit cellular ABCG2 function and resistance to anticancer drug substrates, but not in the parental cells that do not express ABCG2. Sorafenib (up to 2.5 $\mu\text{mol/L}$ concentration in our study) seems to have little effects on 2 other major MDR-ABC transporters (ABCB1 and ABCC1) mediating drug efflux and resistance. In addition to inhibiting ABCG2 function, sorafenib also accelerate its lysosome-dependent degradation. Sorafenib seems to have the same action as previous reported dynamic ABCG2 inhibitors, although different from the previously known Ko143 and TKIs, such as lapatinib or erlotinib, only by inhibiting the efflux function of ABCG2 transporter. On the basis of many ABCG2 degradation-induced inhibitors previously identified, a pharmaco-

phore model was developed and led us to conclude that sorafenib behaves like ABCG2 degradation-induced inhibitor. Sorafenib may, therefore, be a good candidate for MDR chemosensitizing agent. The successful identification of sorafenib as an ABCG2 inhibitor through a pharmacophore-based evaluation process indicates that this is a valuable approach to rediscover novel uses for known drugs and offers new strategies for the reversal of ABCG2-mediated drug transport and resistance.

Disclosure of Potential Conflicts of Interest

No potential conflicts of interest were disclosed.

Authors' Contributions

Conception and design: Y. Wei, Y. Ma, T. Hou, H. Peng
Development of methodology: Q. Zhao, Z. Ren, T. Hou, H. Peng
Acquisition of data (provided animals, acquired and managed patients, provided facilities, etc.): Y. Wei, Y. Ma, T. Hou, H. Peng
Analysis and interpretation of data (e.g., statistical analysis, biostatistics, computational analysis): Y. Wei, Y. Li, T. Hou, H. Peng
Writing, review, and/or revision of the manuscript: Y. Wei, Q. Zhao, T. Hou, H. Peng
Administrative, technical, or material support (i.e., reporting or organizing data, constructing databases): Y. Wei, Y. Ma, T. Hou, H. Peng
Study supervision: Y. Ma, H. Peng

Acknowledgments

The authors thank Prof. Jian-ting Zhang (IU Simon Cancer Center, Indianapolis, IN) for their generous gifts of HEK293-derived cell lines and Prof. Dongsheng Xiong (Institute of Hematology & Blood Diseases Hospital, CAMS & PUMC, China) for providing K562-derived cell lines. The human breast cancer cell line MCF-7 and the mitoxantrone-selected MDR cell line MCF-7/MX were kindly provided by Dr. Erasmus Schneider (Wadsworth Center, Albany, NY). The authors also thank Prof. Jian-ting Zhang, Yihua Zhang, and Jizhen Lin for critical review of the manuscript.

Grant Support

This work was supported by the National Natural Science Foundation of China grant nos. 30873083, 81173082 (H. Peng), and 21173156 (T. Hou) and by the Priority Academic Program Development of Jiangsu Higher Education Institutions (PAPD).

The costs of publication of this article were defrayed in part by the payment of page charges. This article must therefore be hereby marked *advertisement* in accordance with 18 U.S.C. Section 1734 solely to indicate this fact.

Received February 26, 2012; revised May 1, 2012; accepted May 2, 2012; published OnlineFirst May 16, 2012.

References

- Szakács G, Paterson JK, Ludwig JA, Booth-Genthe C, Gottesman MM. Targeting multidrug resistance in cancer. *Nat Rev Drug Discov* 2006;5:219–34.
- Zhang JT. Biochemistry and pharmacology of the human multidrug resistance gene product, ABCG2. *Zhong Nan Da Xue Xue Bao Yi Xue Ban* 2007;32:531–41.
- Robey RW, Ierano C, Zhan Z, Bates SE. The challenge of exploiting ABCG2 in the clinic. *Curr Pharm Biotechnol* 2011;12:595–608.
- Xu J, Peng H, Zhang JT. Human multidrug transporter ABCG2, a target for sensitizing drug resistance in cancer chemotherapy. *Curr Med Chem* 2007;14:689–701.
- He M, Wei MJ. Reversing multidrug resistance by tyrosine kinase inhibitors. *Chin J Cancer* 2012;31:126–33.
- Mi YJ, Liang YJ, Huang HB, Zhao HY, Wu CP, Wang F, et al. Apatinib (YN968D1) reverses multidrug resistance by inhibiting the efflux function of multiple ATP-binding cassette transporters. *Cancer Res* 2010;70:7981–91.
- Dai CL, Liang YJ, Wang YS, Tiwari AK, Yan YY, Wang F, et al. Sensitization of ABCG2-overexpressing cells to conventional chemotherapeutic agent by sunitinib was associated with inhibiting the function of ABCG2. *Cancer Lett* 2009;279:74–83.
- Dai C, Tiwari AK, Wu CP, Su X, Wang SR, Liu D, et al. Lapatinib (Tykerb, GW572016) reverses multidrug resistance in cancer cells by inhibiting the activity of ATP-binding cassette subfamily B member 1 and G member 2. *Cancer Res* 2008;68:7905.
- Shi Z, Peng XX, Kim IW, Shukla S, Si QS, Robey RW, et al. Erlotinib (Tarceva, OSI-774) antagonizes ATP-binding cassette subfamily B member 1 and ATP-binding cassette subfamily G member 2-mediated drug resistance. *Cancer Res* 2007;67:11012–20.
- Nakamura Y, Oka M, Soda H, Shiozawa K, Yoshikawa M, Itoh A, et al. Gefitinib ("Iressa", ZD1839), an epidermal growth factor receptor tyrosine kinase inhibitor, reverses breast cancer resistance protein/ABCG2-mediated drug resistance. *Cancer Res* 2005;65:1541–6.
- Liu W, Baer MR, Bowman MJ, Pera P, Zheng X, Morgan J, et al. The tyrosine kinase inhibitor imatinib mesylate enhances the efficacy of photodynamic therapy by inhibiting ABCG2. *Clin Cancer Res* 2007;13:2463–70.

12. Tiwari AK, Sodani K, Wang SR, Kuang YH, Ashby CR Jr., Chen X, et al. Nilotinib (AMN107, Tasigna) reverses multidrug resistance by inhibiting the activity of the ABCB1/Pgp and ABCG2/BCRP/MXR transporters. *Biochem Pharmacol* 2009;78:153–61.
13. Zheng L, Wang F, Li Y, Zhang X, Chen L, Liang Y, et al. Vandetanib (Zactima, ZD6474) antagonizes ABCG1-and ABCG2-mediated multidrug resistance by inhibition of their transport function. *PLoS One* 2009;4:e5172.
14. Wang XK, Fu LW. Interaction of tyrosine kinase inhibitors with the MDR-related ABC transporter proteins. *Curr Drug Metab* 2010;11:618–28.
15. Peng H, Dong Z, Qi J, Yang Y, Liu Y, Li Z, et al. A novel two mode-acting inhibitor of ABCG2-mediated multidrug transport and resistance in cancer chemotherapy. *PLoS One* 2009;4:e5676.
16. Peng H, Qi J, Dong Z, Zhang JT. Dynamic vs static ABCG2 inhibitors to sensitize drug resistant cancer cells. *PLoS One* 2010;5:e15276.
17. Yang CZ, Luan FJ, Xiong DS, Liu BR, Xu YF, Gu KS. Multidrug resistance in leukemic cell line K562/A02 induced by doxorubicin. *Zhongguo Yao Li Xue Bao* 1995;16:333–7.
18. Xu J, Peng H, Chen Q, Liu Y, Dong Z, Zhang JT. Oligomerization domain of the multidrug resistance-associated transporter ABCG2 and its dominant inhibitory activity. *Cancer Res* 2007;67:4373–81.
19. Yang Y, Chen Q, Zhang JT. Structural and functional consequences of mutating cysteine residues in the amino terminus of human multidrug resistance-associated protein 1. *J Biol Chem* 2002;277:44268–77.
20. Xu J, Liu Y, Yang Y, Bates S, Zhang JT. Characterization of oligomeric human half-ABC transporter ATP-binding cassette G2. *J Biol Chem* 2004;279:19781–9.
21. Volk EL, Farley KM, Wu Y, Li F, Robey RW, Schneider E. Overexpression of wild-type breast cancer resistance protein mediates methotrexate resistance. *Cancer Res* 2002;62:5035–40.
22. Henrich CJ, Robey RW, Bokesch HR, Bates SE, Shukla S, Ambudkar SV, et al. New inhibitors of ABCG2 identified by high-throughput screening. *Mol Cancer Ther* 2007;6:3271–8.
23. Lacerda L, Pusztai L, Woodward WA. The role of tumor initiating cells in drug resistance of breast cancer: Implications for future therapeutic approaches. *Drug Resist Updat* 2010;13:99–108.
24. Broxterman HJ, Gotink KJ, Verheul HM. Understanding the causes of multidrug resistance in cancer: a comparison of doxorubicin and sunitinib. *Drug Resist Updat* 2009;12:114–26.
25. Agarwal S, Sane R, Ohlfest JR, Elmquist WF. The role of the breast cancer resistance protein (ABCG2) in the distribution of sorafenib to the brain. *J Pharmacol Exp Ther* 2011;336:223–33.
26. Lagas JS, van Waterschoot RA, Sparidans RW, Wagenaar E, Beijnen JH, Schinkel AH. Breast cancer resistance protein and P-glycoprotein limit sorafenib brain accumulation. *Mol Cancer Ther* 2010;9:319–26.
27. Hu S, Chen Z, Franke R, Orwick S, Zhao M, Rudek MA, et al. Interaction of the multikinase inhibitors sorafenib and sunitinib with solute carriers and ATP-binding cassette transporters. *Clin Cancer Res* 2009;15:6062–9.
28. Poller B, Wagenaar E, Tang SC, Schinkel AH. Double-transduced MDCKII cells to study human P-glycoprotein (ABCB1) and breast cancer resistance protein (ABCG2) interplay in drug transport across the blood-brain barrier. *Mol Pharm* 2011;8:571–82.
29. Hegedus C, Ozvegy-Laczka C, Szakacs G, Sarkadi B. Interaction of ABC multidrug transporters with anticancer protein kinase inhibitors: substrates and/or inhibitors? *Curr Cancer Drug Targets* 2009;9:252–72.
30. Blanchet B, Billemont B, Cramard J, Benichou AS, Chhun S, Harcouet L, et al. Validation of an HPLC-UV method for sorafenib determination in human plasma and application to cancer patients in routine clinical practice. *J Pharm Biomed Anal* 2009;49:1109–14.

Molecular Cancer Therapeutics

New Use for an Old Drug: Inhibiting ABCG2 with Sorafenib

Yinxiang Wei, Yuanfang Ma, Qing Zhao, et al.

Mol Cancer Ther 2012;11:1693-1702. Published OnlineFirst May 16, 2012.

Updated version Access the most recent version of this article at:
doi:[10.1158/1535-7163.MCT-12-0215](https://doi.org/10.1158/1535-7163.MCT-12-0215)

Supplementary Material Access the most recent supplemental material at:
<http://mct.aacrjournals.org/content/suppl/2012/05/16/1535-7163.MCT-12-0215.DC1>

Cited articles This article cites 30 articles, 13 of which you can access for free at:
<http://mct.aacrjournals.org/content/11/8/1693.full#ref-list-1>

Citing articles This article has been cited by 3 HighWire-hosted articles. Access the articles at:
<http://mct.aacrjournals.org/content/11/8/1693.full#related-urls>

E-mail alerts [Sign up to receive free email-alerts](#) related to this article or journal.

Reprints and Subscriptions To order reprints of this article or to subscribe to the journal, contact the AACR Publications Department at pubs@aacr.org.

Permissions To request permission to re-use all or part of this article, use this link
<http://mct.aacrjournals.org/content/11/8/1693>.
Click on "Request Permissions" which will take you to the Copyright Clearance Center's (CCC) Rightslink site.